Strong polarization mode coupling in microresonators

Sven Ramelow,[1,2,*] Alessandro Farsi,[1] Stéphane Clemmen,[1] Jacob S. Levy,[3] Adrea R. Johnson,[1] Yoshitomo Okawachi,[1] Michael. R. E. Lamont,[1,4] Michal Lipson,[3,4] and Alexander L. Gaeta[1,4]

[1]*School of Applied and Engineering Physics, Cornell University, Ithaca, New York 14853, USA*

[2]*Faculty of Physics, University of Vienna, 1090 Vienna, Austria*

[3]*School of Electrical and Computer Engineering, Cornell University, Ithaca, New York 14853, USA*

[4]*Kavli Institute at Cornell for Nanoscale Science, Cornell University, Ithaca, New York 14853, USA*

**Corresponding author: sven.ramelow@univie.ac.at*

Received May 20, 2014; revised July 23, 2014; accepted July 28, 2014;
posted July 28, 2014 (Doc. ID 212505); published August 25, 2014

We observe strong modal coupling between the TE_{00} and TM_{00} modes in Si_3N_4 ring resonators revealed by avoided crossings of the corresponding resonances. Such couplings result in significant shifts of the resonance frequencies over a wide range around the crossing points. This leads to an effective dispersion that is one order of magnitude larger than the intrinsic dispersion and creates broad windows of anomalous dispersion. We also observe the changes to frequency comb spectra generated in Si_3N_4 microresonators due to polarization mode and higher-order mode crossings and suggest approaches to avoid these effects. Alternatively, such polarization mode crossings can be used as a tool for dispersion engineering in microresonators.

OCIS codes: (190.4380) Nonlinear optics, four-wave mixing; (190.4390) Nonlinear optics, integrated optics; (140.4780) Optical resonators; (130.3990) Micro-optical devices.

http://dx.doi.org/10.1364/OL.39.005134

Optical microresonators are important for a wide range of applications, such as parametric frequency combs [1–10], optomechanics [11,12], and in quantum optics as sources for photon pairs [13–19] or squeezed states [20,21]. The microresonator resonances can in principle be precisely calculated using the dispersion of the resonating modes and the resonator length. However, modal coupling between different types of modes can significantly alter the shape and position of their resonances. Mode splitting occurs for strong coupling [22], and coupling between whole families of modes results in avoided crossings [23–28]. Avoided crossings occur in resonators when two distinct, frequency-degenerate modes are coupled and form new eigenmodes. The frequencies of these eigenmodes are no longer degenerate with a splitting proportional to the coupling strength resulting in the absence of a crossing of the eigenmode resonances. In microresonators this behavior can lead to dramatic localized changes in the effective dispersion near these crossing points, which in general affects any parametric interaction that relies on precise frequency matching of different resonances. In particular it can play an important role in the formation of parametric frequency combs [24–32]. While mode crossings can be disruptive for comb generation by inhibiting soliton formation [25] and distorting the comb spectrum [27], they can also be beneficial, allowing for comb formation in resonators with normal group-velocity dispersion (GVD) [8,24] or aiding the generation of dark solitons in normal GVD resonators [30]. In the context of frequency comb generation, only modal interactions between different families of spatial modes have been considered thus far. However, in dielectric waveguides, even when the waveguide is "single mode," there are typically at least two guided fundamental modes: the fundamental quasi-transverse electric (TE_{00}) and the fundamental quasi-transverse magnetic (TM_{00}) mode, which correspond approximately to the polarization of light in the waveguide.

Here, we report on the observation of avoided crossings that result from the strong modal coupling between the TE_{00} and TM_{00} polarization modes in Si_3N_4 microring resonators. Similarly strong polarization mode coupling has been shown to be useful for polarization conversion based on silicon oxynitride technology [32]. Since such a mode interaction can even occur in single-mode waveguides, it is more universal than other forms of modal interactions (i.e., between higher-order spatial modes). The physical origin and strength of the modal coupling between the TE_{00} and TM_{00} modes are based on different parameters of the ring resonator, such as its radius of curvature, waveguide cross section, and side-wall angle [33,34]. While in most cases the polarization properties follow from the corresponding straight-waveguide characteristics [35], microresonators with smaller bend radii and larger side-wall angles typically will exhibit greater modal coupling.

Our experimental setup for investigating polarization mode coupling is depicted in Fig. 1. We probe the resonators with two different external-cavity diode lasers covering a total tuning range between 1450 and 1640 nm. Lensed fibers are used to couple into and out of the bus waveguide with inverted tapers [36] for mode matching. The polarization of the input and output light is controlled and analyzed with standard fiber-based polarization controllers and a polarization beam splitter, and the output power is monitored with a sensitive photodiode. We use a temperature controller with a Peltier element on the chip holder to stabilize and tune the Si_3N_4 microring resonators under investigation. To overcome the limited precision of our tunable lasers, we use an automated stepped scanning and fitting routine supplemented by calibrating each resonance position with a high-precision wavemeter. We find that this method leads to an average precision better than 50 MHz.

We first investigate polarization mode coupling in two Si_3N_4 microrings with 725 nm × 1100 nm and 725 nm × 900 nm waveguide cross sections (effective refractive

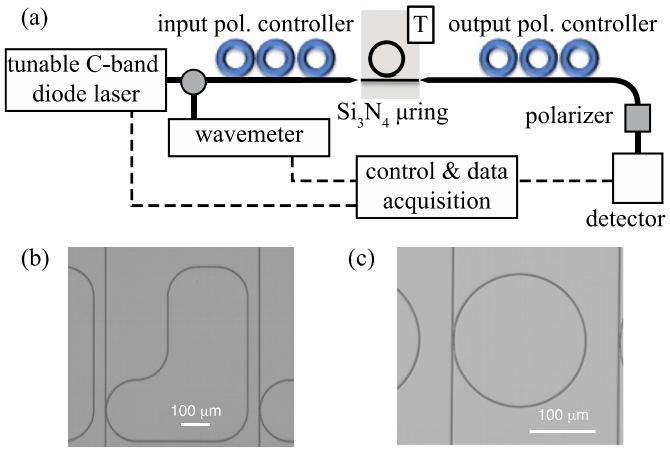

Fig. 1. (a) Schematic of the setup used for observing and characterizing polarization mode coupling in mircoresonators on a temperature stabilized (T) silicon chip. (b), (c) SEM images of the microresonators and the coupling regions with the bus waveguides for (b) the 1.8 mm long microresonator and (c) a 100 μm radius ring resonator.

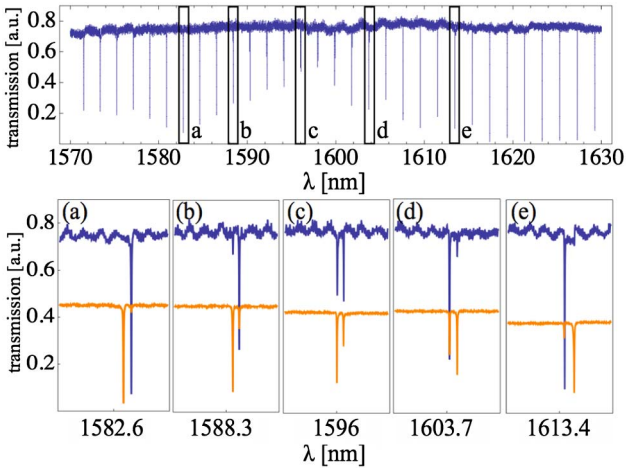

Fig. 2. Optical transmission for TM_{00} polarized light and selected resonances (a)–(e) in detail for TM_{00} (blue) and TE_{00} (orange). The appearance of the TE_{00} resonances for TM_{00} polarized input (and vice versa) and their behavior indicate an avoided crossing near 1595 nm.

index of 1.7 for both), 100 μm radii, and 10° side-wall angles. The transmission measurement for TM_{00} input light for the first microring (Fig. 2) yields sharp and deep resonances due to nearly critical coupling between the bus waveguide and the resonator. Near 1595 nm, a second sharp resonance, which we associate with the TE_{00} mode, appears on the right side of the main TM_{00} resonance and becomes deeper until both show the same extinction. The main resonance then experiences an adiabatic crossover and the secondary resonance (now on the left side) slowly disappears. We attribute this behavior to an avoided crossing at 1595 nm associated with a strong modal interaction between the TE_{00} and TM_{00} modes. We verify this by a number of different measurements. First, we observe that the adiabatic crossover behavior is inverted when the initial input is TE_{00} polarized. Additionally, we verified that the eigenmodes at the crossing are fully hybridized being a superposition of the TE_{00} and TM_{00} polarization.

To observe the avoided crossing associated with the strong polarization mode coupling, we next precisely measured the resonance wavelengths for both the TE_{00} and TM_{00} polarizations as shown in Fig. 3. For the first microring, the measured free spectral ranges (FSRs) at the start of the scan (1510 nm) are 225.0 and 226.3 GHz for the TM_{00} and TE_{00} modes, respectively. This agrees very well with the FSRs calculated from the simulated dispersion based on a finite-element mode solver [also shown in Fig. 2(b)] and therefore further corroborates the identification of the modes as TM_{00} and TE_{00}.

As shown in Fig. 3(a), a strong avoided crossing occurs near 1595 nm with the upper branch (blue) changing its mode character continuously from TE_{00} to TM_{00} and vice versa for the second branch. We find a similarly strong avoided crossing for the microring with a 725 nm × 900 nm waveguide cross section [Fig. 3(d)]. The splittings of the modes at the anticrossings is 7.2 and 12.5 GHz. For both resonators this is around 20 times larger than their intrinsic loss rates, which we measure to be 340 MHz ($Q_{\mathrm{int}} \approx 600,000$) and 700 MHz ($Q_{\mathrm{int}} \approx 300,000$), and shows that for both microrings the TE_{00} and TM_{00} modes are strongly coupled.

As shown in Figs. 3(b) and 3(e), near the crossing points, the measured FSRs deviate significantly from their values given by the dispersion and resonator length.

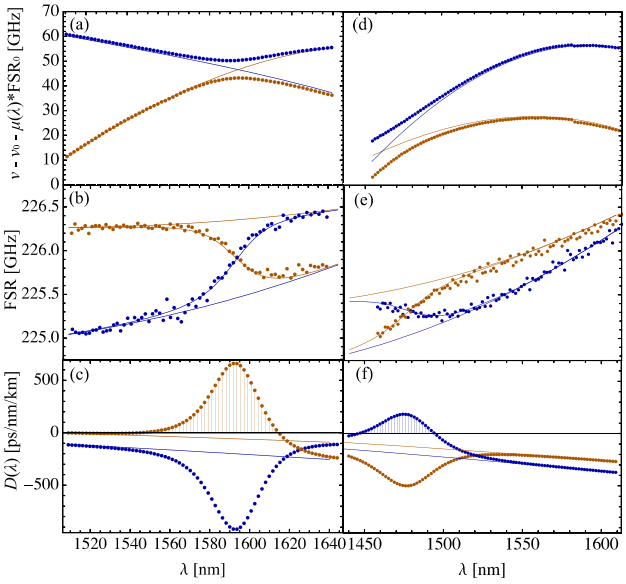

Fig. 3. Polarization avoided crossings for two Si_3N_4 microrings with 725 nm × 1100 nm cross section [(a)–(c)] and 725 nm × 900 nm cross section [(d)–(f)]. (a), (d) Measured resonance frequencies ν of the TE_{00} and TM_{00} modes parameterized by their relative mode number μ, a constant $FSR_0 = 226$ GHz, and an offset frequency of $\nu_0 = c/1509.2$ nm for (a) and $\nu_0 = c/1456.4$ nm for (d). The solid lines show the theoretical TE_{00} and TM_{00} resonance frequencies based on simulations of the eigenmodes inside the resonator without accounting for the modal interaction. (b), (e) Measured FSRs (dotted lines), fits to the measured data (solid lines), and the simulation results. (c), (f) Experimentally determined effective GVD (dotted lines) derived from the fits to the measured data in (b) and (e), respectively, and simulation results yielding the intrinsic GVD (solid lines).

This can be interpreted as a mode-coupling-induced effective dispersion [8]. By fitting the function for FSR(λ) for each of the different branches, the values of the effective GVD can be directly determined from the measured data [Figs. 3(c) and 3(f)] through the relation $\mathrm{GVD}(\lambda) = \partial/\partial\lambda(1/\mathrm{FSR}(\lambda)/L)$.

For the first microring, we observe relatively high values of the effective GVD reaching around +600 ps/nm/km and −900 ps/nm/km. Moreover, for the TE_{00} branch (that turns into TM_{00} after the crossing), there is a wide range between 1550 and 1610 nm of anomalous GVD. We measure a similar effect on the effective GVD in the second microring [Fig. 3(f)] with an anomalous GVD region between 1450 and 1495 nm.

We further investigate the effects of both polarization and higher-order mode crossings on comb generation by directly comparing the comb spectra generated in microring resonators with a measurement of its mode crossings (Fig. 4). The combs are generated by strongly pumping a single resonance at 1540 nm [4]. We investigate a microring resonator with a waveguide cross section of 725 nm × 1650 nm (effective refractive index of 1.8), a 100 μm radius, and a 10° side-wall angle [Fig. 4(a)]. We observe a polarization mode crossing near

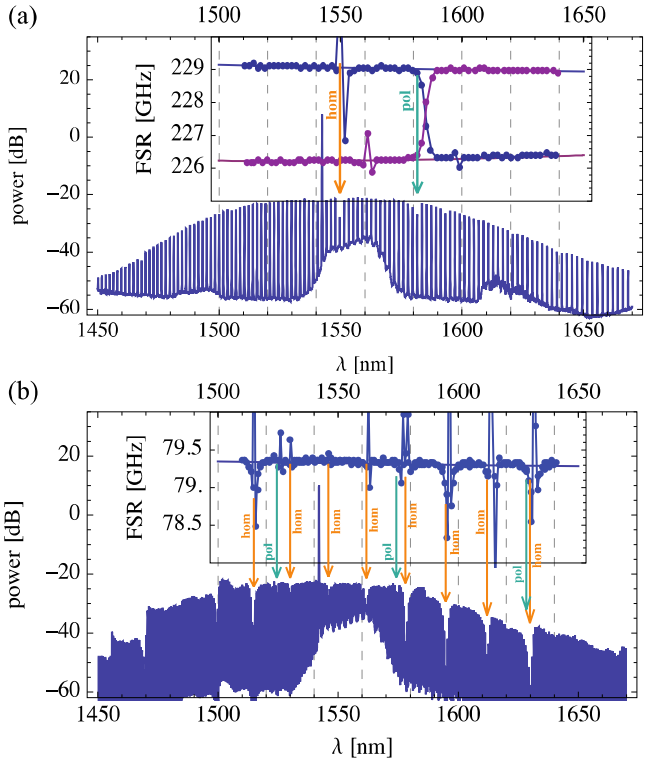

Fig. 4. Generated comb spectra in Si_3N_4 microresonators. Insets show the measured FSRs with the (upper) blue branch being for the TE_{00} mode and revealing the mode crossings. (a) Results for a 725 nm × 1650 nm cross section, 100 μm radius microring resonator. A polarization mode crossing (pol) occurs near 1580 nm with a corresponding feature (indicated by an arrow) in the comb spectrum. A second anomaly in the FSRs near 1550 nm due to a mode crossing with a higher-order spatial mode (hom) also produces a corresponding feature in the spectrum. (b) Results for a 725 nm × 1700 nm cross section, 1.8 mm length microresonator. A number of polarization and higher-order mode crossings affect the generated comb spectrum.

1580 nm with a splitting at the avoided crossing of 2.2 GHz, which greatly exceeds the intrinsic loss rate of the resonator. This polarization mode crossing manifests as a reduction in the mode intensity in the generated comb spectrum. In addition, there exists an anomaly in the FSR at 1550 nm, which can be attributed to a mode crossing with a higher-order spatial mode, and we observe a similar corresponding feature in the comb spectrum. Furthermore, we observe suppressed comb generation when pumping near one of the higher-order mode crossings that we attribute to the large change in the effective dispersion. Since this effect can be disadvantageous for applications related to frequency comb generation, it needs to be taken into account in the optimal device design. Moreover, we investigate the effects of mode crossings on comb generation in an 80 GHz FSR microresonator with a waveguide cross section of 725 nm × 1700 nm (effective refractive index of 1.8), a 1.8 mm length, and a 10° side-wall angle close [Fig. 4(b)]. For this microresonator our measurements reveal three polarization mode crossings and a number of higher-order mode crossings that affect the comb spectrum generated from this resonator.

We identify different strategies that could minimize the disruptive effects of mode-crossings (polarization and higher-order mode) on frequency comb generation. In general, mode crossings are especially disruptive when they appear directly at the pump wavelength or when they line up symmetrically with respect to the pump since they will then simultaneously affect both the signal and idler resonances. Since the position of any mode crossing depends sensitively on the exact length of the microresonators, slight variations in the design of the resonator lengths can be used to circumvent both scenarios. In addition, if the target application allows it, increasing the FSR will reduce the frequency at which mode crossings will occur. Another approach for reducing mode-crossing disruptions would be to minimize the modal interactions altogether, which may be achieved by optimizing the microresonator design and fabrication, including larger bend radii or smaller side-wall angles. Furthermore, we have observed experimentally that higher-order mode crossings are suppressed for the narrower and thus more symmetric cross-section resonators (Fig. 3), as compared to the wider, more asymmetric cross-section resonators (Fig. 4). This indicates that the aspect ratio can be used as an additional parameter for controlling mode-crossing effects.

In summary, we observe and characterize strong avoided crossings between the TE_{00} and TM_{00} resonance frequencies in Si_3N_4 microresonators and study their effect on effective GVD and frequency comb generation. We believe there are several interesting applications of strong polarization crossings. First, for certain applications, such as nondegenerate frequency conversion, involving a strong pump field it is useful to suppress parametric processes solely stimulated by the pump, as this would induce noise for the target process. The frequency mismatch induced by mode crossings can be very strong (we observe an effective GVD as large as 900 ps/nm/km), which can be used for suppression of unwanted parametric processes. In addition, we measure a rather smooth and well-defined change in the effective

dispersion and observe wide windows of anomalous GVD in otherwise normal GVD microresonators. These anomalous GVD windows could allow the generation of parametric frequency combs in such normal GVD resonators. Moreover, the TE_{00} and TM_{00} modes can simultaneously experience significantly lower loss than the higher-order modes. The exact position of polarization mode crossings can be controlled by accurately designing the cavity length. Thus, while avoided crossings may be disruptive for certain applications, these polarization mode crossings can be a useful dispersion engineering tool to tailor and optimize microresonator frequency matching for a wide range of parametric processes underlying frequency comb generation and other microresonator applications.

We acknowledge support from the Defense Advanced Research Projects Agency via the QuASAR program and the Air-Force Office of Scientific Research under grant FA9550-12-1-0377 and Semiconductor Research Corporation. This work was performed in part at the Cornell Nano-Scale Facility, a member of the National Nanotechnology Infrastructure Network, which is supported by the National Science Foundation (grant ECS-0335765). SR is funded by a EU Marie-Curie Fellowship (PIOF-GA-2012-329851).

References

1. P. Del'Haye, A. Schliesser, O. Arcizet, T. Wilken, R. Holzwarth, and T. J. Kippenberg, Nature **450**, 1214 (2007).
2. A. A. Savchenkov, A. B. Matsko, V. S. Ilchenko, I. Solomatine, D. Seidel, and L. Maleki, Phys. Rev. Lett. **101**, 093902 (2008).
3. M. A. Foster, J. S. Levy, O. Kuzucu, K. Saha, M. Lipson, and A. L. Gaeta, Opt. Express **19**, 14233 (2011).
4. Y. Okawachi, K. Saha, J. S. Levy, Y. H. Wen, M. Lipson, and A. L. Gaeta, Opt. Lett. **36**, 3398 (2011).
5. W. Liang, A. A. Savchenkov, A. B. Matsko, V. S. Ilchenko, D. Seidel, and L. Maleki, Opt. Lett. **36**, 2290 (2011).
6. S. B. Papp and S. A. Diddams, Phys. Rev. A **84**, 053833 (2011).
7. F. Ferdous, H. Miao, D. E. Leaird, K. Srinivasan, J. Wang, L. Chen, L. T. Varghese, and A. M. Weiner, Nat. Photonics **5**, 770 (2011).
8. T. Herr, K. Hartinger, J. Riemensberger, C. Y. Wang, E. Gavartin, R. Holzwarth, M. L. Gorodetsky, and T. J. Kippenberg, Nat. Photonics **6**, 480 (2012).
9. K. Saha, Y. Okawachi, B. Shim, J. S. Levy, R. Salem, A. R. Johnson, M. A. Foster, M. R. E. Lamont, M. Lipson, and A. L. Gaeta, Opt. Express **21**, 1335 (2013).
10. T. J. Kippenberg, R. Holzwarth, and S. A. Diddams, Science **332**, 555 (2011).
11. T. J. Kippenberg and K. J. Vahala, Science **321**, 1172 (2008).
12. M. Aspelmeyer, T. J. Kippenberg, and F. Marquardt, "Cavity optomechanics," arXiv:1303.0733 (2013).
13. S. Clemmen, K. Phan Huy, W. Bogaerts, R. G. Baets, Ph. Emplit, and S. Massar, Opt. Express **17**, 16558 (2009).
14. S. Clemmen, A. Farsi, J. Levy, L. Helt, M. Liscidini, J. Sipe, M. Lipson, and A. L. Gaeta, in *Frontiers in Optics/Laser Science XXVII*, OSA Technical Digest (Optical Society of America, 2011), paper FThE5.
15. S. Azzini, D. Grassani, M. J. Strain, M. Sorel, L. G. Helt, J. E. Sipe, M. Liscidini, M. Galli, and D. Bajoni, Opt. Express **20**, 23100 (2012).
16. W. C. Jiang, X. Lu, J. Zhang, O. Painter, and Q. Lin, "A silicon-chip source of bright photon-pair comb," arXiv:1210.4455 (2012).
17. R. Kumar, J. R. Ong, J. Recchio, K. Srinivasan, and S. Mookherjea, Opt. Lett. **38**, 2969 (2013).
18. C. Reimer, L. Caspani, M. Clerici, M. Ferrera, M. Kues, M. Peccianti, A. Pasquazi, L. Razzari, B. E. Little, S. T. Chu, D. J. Moss, and R. Morandotti, Opt. Express **22**, 6535 (2014).
19. M. Förtsch, J. Fürst, C. Wittmann, D. Strekalov, A. Aiello, M. V. Chekhova, C. Silberhorn, G. Leuchs, and C. Marquardt, Nat. Commun. **4**, 1818 (2013).
20. A. H. Safavi-Naeini, S. Gröblacher, J. T. Hill, J. Chan, M. Aspelmeyer, and O. Painter, Nature **500**, 185 (2013).
21. A. Dutt, K. Luke, S. Manipatruni, A. L. Gaeta, P. Nussenzveig, and M. Lipson, "On-chip optical squeezing," arXiv: 1309.6371 (2013).
22. T. J. Kippenberg, S. M. Spillane, and K. J. Vahala, Opt. Lett. **27**, 1669 (2002).
23. T. Carmon, H. G. L. Schwefel, L. Yang, M. Oxborrow, A. D. Stone, and K. J. Vahala, Phys. Rev. Lett. **100**, 103905 (2008).
24. A. A. Savchenkov, A. B. Matsko, W. Liang, V. S. Ilchenko, D. Seidel, and L. Maleki, Opt. Express **20**, 27290 (2012).
25. T. Herr, V. Brasch, J. D. Jost, I. Mirgorodskiy, G. Lihachev, M. L. Gorodetsky, and T. J. Kippenberg, "Mode spectrum and temporal soliton formation in optical microresonators," arXiv:1311.1716 (2013).
26. Y. Liu, Y. Xuan, X. Xue, P.-H. Wang, A. J. Metcalf, S. Chen, M. Qi, and A. M. Weiner, "Investigation of mode interaction in optical microresonators for Kerr frequency comb generation," arXiv:1402.5686 (2014).
27. I. S. Grudinin, L. Baumgartel, and N. Yu, Opt. Express **21**, 26929 (2013).
28. F. Sedlmeir, M. Hauer, J. U. Fürst, G. Leuchs, and H. G. L. Schwefel, Opt. Express **21**, 23942 (2013).
29. I. S. Grudinin, L. Baumgartel, and N. Yu, Opt. Express **20**, 6604 (2012).
30. X. Xue, Y. Xuan, Y. Liu, P.-H. Wang, S. Chen, J. Wang, D. E. Leaird, M. Qi, and A. M. Weiner, "Mode interaction aided soft excitation of dark solitons in normal dispersion microresonators and offset-frequency tunable Kerr combs," arXiv:1404.2865 (2014).
31. S.-W. Huang, J. F. McMillan, J. Yang, A. Matsko, H. Zhou, M. Yu, D.-L. Kwong, L. Maleki, and C. W. Wong, "Direct generation of 74-fs mode-locking from on-chip normal dispersion frequency combs," arXiv:1404.3256 (2014).
32. A. Melloni, F. Morichetti, and M. Martinelli, Opt. Lett. **29**, 2785 (2004).
33. W. W. Lui, T. Hirono, K. Yokoyama, and W. Huang, J. Lightwave Technol. **16**, 929 (1998).
34. N. Somasiri and B. M. A. Rahman, J. Lightwave Technol. **21**, 54 (2003).
35. F. Morichetti, A. Melloni, and M. Martinelli, in *International Conference on Transparent Optical Networks* (IEEE, 2006), Vol. **4**, p. 261.
36. V. R. Almeida, R. R. Panepucci, and M. Lipson, Opt. Lett. **28**, 1302 (2003).